Interference Effect between ϕ and $\Lambda(1520)$ Production Channels in the $\gamma p \to K^+K^-p$ Reaction near Threshold

S. Y. Ryu,[1] J. K. Ahn,[2] T. Nakano,[1] D. S. Ahn,[3] S. Ajimura,[1] H. Akimune,[4] Y. Asano,[5] W. C. Chang,[6] J. Y. Chen,[7] S. Daté,[8] H. Ejiri,[1] H. Fujimura,[9] M. Fujiwara,[1] S. Fukui,[1] S. Hasegawa,[1] K. Hicks,[10] K. Horie,[11] T. Hotta,[1] S. H. Hwang,[12] K. Imai,[13] T. Ishikawa,[14] T. Iwata,[15] Y. Kato,[16] H. Kawai,[17] K. Kino,[1] H. Kohri,[1] Y. Kon,[1] N. Kumagai,[8] P. J. Lin,[6] Y. Maeda,[18] S. Makino,[9] T. Matsuda,[19] N. Matsuoka,[1] T. Mibe,[20] M. Miyabe,[14] M. Miyachi,[21] Y. Morino,[20] N. Muramatsu,[14] R. Murayama,[11] Y. Nakatsugawa,[20] S. i. Nam,[22] M. Niiyama,[23] M. Nomachi,[1] Y. Ohashi,[8] H. Ohkuma,[8] T. Ohta,[1] T. Ooba,[17] D. S. Oshuev,[6] J. D. Parker,[23] C. Rangacharyulu,[24] A. Sakaguchi,[11] T. Sawada,[6] P. M. Shagin,[25] Y. Shiino,[17] H. Shimizu,[14] E. A. Strokovsky,[26,*] Y. Sugaya,[1] M. Sumihama,[27] A. O. Tokiyasu,[14] Y. Toi,[19] H. Toyokawa,[8] T. Tsunemi,[23] M. Uchida,[21] M. Ungaro,[28] A. Wakai,[29] C. W. Wang,[6] S. C. Wang,[6] K. Yonehara,[4] T. Yorita,[1] M. Yoshimura,[30] M. Yosoi,[1] and R. G. T. Zegers[31]

(LEPS Collaboration)

[1]*Research Center for Nuclear Physics, Osaka University, Ibaraki, Osaka 567-0047, Japan*
[2]*Department of Physics, Korea University, Seoul 02841, Republic of Korea*
[3]*RIKEN, The Institute of Physical and Chemical Research, Wako, Saitama 351-0198, Japan*
[4]*Department of Physics, Konan University, Kobe, Hyogo 658-8501, Japan*
[5]*XFEL Project Head Office, RIKEN, Sayo, Hyogo 679-5143, Japan*
[6]*Institute of Physics, Academia Sinica, Taipei 11529, Taiwan*
[7]*Light Source Division, National Synchrotron Radiation Research Center, Hsinchu 30076, Taiwan*
[8]*Japan Synchrotron Radiation Research Institute, Sayo, Hyogo 679-5143, Japan*
[9]*Wakayama Medical College, Wakayama 641-8509, Japan*
[10]*Department of Physics and Astronomy, Ohio University, Athens, Ohio 45701, USA*
[11]*Department of Physics, Osaka University, Toyonaka, Osaka 560-0043, Japan*
[12]*Korea Research Institute of Standards and Science (KRISS), Daejeon 34113, Republic of Korea*
[13]*Advanced Science Research Center, Japan Atomic Energy Agency, Tokai, Ibaraki 319-1195, Japan*
[14]*Research Center for Electron Photon Science, Tohoku University, Sendai, Miyagi 982-0826, Japan*
[15]*Department of Physics, Yamagata University, Yamagata 990-8560, Japan*
[16]*Kobayashi-Maskawa Institute, Nagoya University, Nagoya, Aichi 464-8602, Japan*
[17]*Department of Physics, Chiba University, Chiba 263-8522, Japan*
[18]*Proton Therapy Center, Fukui Prefectural Hospital, Fukui 910-8526, Japan*
[19]*Department of Applied Physics, Miyazaki University, Miyazaki 889-2192, Japan*
[20]*High Energy Accelerator Organization (KEK), Tsukuba, Ibaraki 305-0801, Japan*
[21]*Department of Physics, Tokyo Institute of Technology, Tokyo 152-8551, Japan*
[22]*Department of Physics, Pukyong National University, Busan 48513, Republic of Korea*
[23]*Department of Physics, Kyoto University, Kyoto 606-8502, Japan*
[24]*Department of Physics and Engineering Physics, University of Saskatchewan, Saskatoon, Saskatchewan S7N 5E2, Canada*
[25]*School of Physics and Astronomy, University of Minnesota, Minneapolis, Minnesota 55455, USA*
[26]*Joint Institute for Nuclear Research, Dubna, Moscow Region, 142281, Russia*
[27]*Department of Education, Gifu University, Gifu 501-1193, Japan*
[28]*Department of Physics, University of Connecticut, Storrs, Connecticut 06269-3046, USA*
[29]*Akita Research Institute of Brain and Blood Vessels, Akita 010-0874, Japan*
[30]*Institute for Protein Research, Osaka University, Suita, Osaka 565-0871, Japan*
[31]*National Superconducting Cyclotron Laboratory, Michigan State University, East Lansing, Michigan 48824, USA*

(Received 2 March 2016; published 7 June 2016)

The ϕ-$\Lambda(1520)$ interference effect in the $\gamma p \to K^+K^-p$ reaction has been measured for the first time in the energy range from 1.673 to 2.173 GeV. The relative phases between ϕ and $\Lambda(1520)$ production amplitudes were obtained in the kinematic region where the two resonances overlap. The measurement results support strong constructive interference when K^+K^- pairs are observed at forward angles but destructive interference for proton emission at forward angles. Furthermore, the observed interference effect does not account for the $\sqrt{s} = 2.1$ GeV bump structure in forward differential cross sections for ϕ

photoproduction. This fact suggests possible exotic structures such as a hidden-strangeness pentaquark state, a new Pomeron exchange, or rescattering processes via other hyperon states.

DOI: 10.1103/PhysRevLett.116.232001

The ϕ-meson production has the unique feature within gluon dynamics of being a result of Okubo-Zweig-Iizuka suppression due to the dominant $s\bar{s}$ structure of the ϕ meson, which is predicted to proceed via a Pomeron trajectory with $J^{PC} = 0^{++}$ [1–7]. Cross sections for diffractive ϕ photoproduction are then predicted to increase smoothly with photon energy. However, a bump structure at $\sqrt{s} = 2.1$ GeV in forward differential cross sections was first reported by the LEPS Collaboration [8]. Despite extensive experimental efforts devoted for the photoproduction of ϕ mesons near threshold, the nature of the bump structure has not yet been explained in detail [9,10]. Kiswandhi *et al.* [11] suggested that the bump structure is the result of an excitation of missing nucleon resonances. However, the bump structure observed from CLAS appears only at forward angles; thus, a conventional resonance interpretation seems less likely [10]. Very recently, the LHCb Collaboration [12] claimed to have observed two $J/\psi p$ resonances referred to as hidden-charm pentaquark states ($c\bar{c}uud$) from Λ_b^0 decays. In ϕ photoproduction, a hidden-strangeness pentaquark state could also be searched for as a candidate for the forward bump structure. Recent theoretical studies further relate this to a coupling between the ϕp and $K^+\Lambda(1520)$ channels, because the bump structure occurs very close to the threshold of $\Lambda(1520)$ production [13,14]. The ϕ-$\Lambda(1520)$ interference could also account for the bump structure, but it has not yet been measured in K^+K^-p photoproduction. The interference may be either positive (constructive) or negative (destructive), depending on the relative phase between the amplitudes of ϕ and $\Lambda(1520)$ production.

Here, we report on the measurement of forward differential cross sections for ϕ and $\Lambda(1520)$ photoproduction and the relative phase angles between their photoproduction amplitudes. This analysis includes the event selection for $\gamma p \to K^+K^-p$, which was based on a kinematic fit. The yields of ϕ and $\Lambda(1520)$ were obtained from a simultaneous fit of the $m_{K^+K^-}$ and m_{K^-p} invariant masses with line shapes from a Monte Carlo simulation. This self-consistent analysis enables the investigation of interference effects between ϕ and $\Lambda(1520)$. To our knowledge, no interference measurement for this reaction has previously been reported in the literature.

The experiment was carried out using the LEPS detector at the SPring-8 facility in Japan. Linearly polarized photons with energies from 1.5 to 2.4 GeV were produced using a laser backscattering technique [15] with UV lasers. The photon beam was incident on a 15-cm liquid-hydrogen (LH_2) target, in which K^+, K^-, and p particles were produced and then passed through the LEPS spectrometer with the standard configuration [16].

With a full data set of LH_2 runs, an analysis on ϕ-$\Lambda(1520)$ photoproduction was performed using kinematic fits and simultaneous fits on the K^+K^- and K^-p mass spectra with Monte Carlo line shapes. To identify candidate events, at least two of the K^+, K^-, and p tracks were required to be reconstructed using standard particle identification methods.

Mass spectra, calculated from the measured four-vectors of detected K^-, K^+, and p, are shown in Fig. 1. The solid

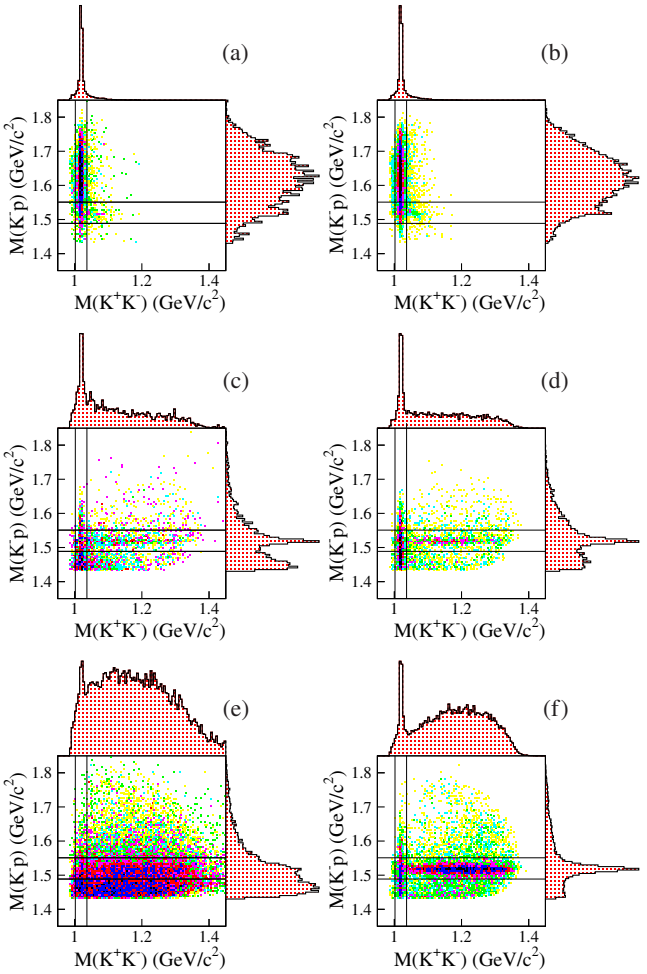

FIG. 1. Top: Scatter plots of the invariant mass of the K^+K^- system versus that of the K^-p system for forward K^-K^+ events (a) before and (b) after the kinematic fit. Middle: The same as the top but for forward K^-p events (c) before and (d) after the kinematic fit. Bottom: The same as the top but for forward K^+p events (e) before and (f) after the kinematic fit. Each scatter plot shows the projections onto each invariant mass axis.

lines represent ϕ and $\Lambda(1520)$ mass bands, each corresponding to a $4\Gamma_\phi$ window for ϕ production and a $2\Gamma_{\Lambda^*}$ window for $\Lambda(1520)$ production, respectively, where $\Gamma_\phi = 4.266$ MeV and $\Gamma_{\Lambda^*} = 15.6$ MeV [17]. Forward particle pairs correspond to the pairs mostly produced in the range of $\cos\theta^* > 0.5$, where θ^* is the angle between the pair and the beam axis in the production center of mass system.

The kinematic fit reconstructs three unmeasured parameters for a missing particle in the K^-K^+p final state. The energy and momentum conservation laws provide four constraints. Consequently, we have an overdetermined system with four constraints and three unknowns. When the χ^2 probability of kinematic fit is required to be greater than 2%, clear ϕ and $\Lambda(1520)$ bands are seen in the $M(K^+K^-)$ versus the $M(K^-p)$ plots [see Figs. 1(b), 1(d), and 1(f)]. For forward K^+p events [Fig. 1(e)], the background primarily represents a $K^{*0}\Sigma^+$ production channel with a small contribution from the $K^+\Lambda(1520)$ channel, followed by the $\Lambda(1520) \to \Sigma^+\pi^-$ decay. However, very little K^* background remains after a kinematic fit is applied [as shown by the histogram in Fig. 1(f)].

The measured K^+K^- and K^-p mass spectra for the selected K^+K^-p events were fitted with line shapes from simulated processes of the ϕp [18], $\Lambda(1520)K^+$ [19], and nonresonant K^+K^-p channels. For events in which K^+p is detected, these mass spectra are fitted with the three processes as well as $K^{*0}\Sigma^+$ [20] and $K^+[\Lambda(1520) \to \Sigma^+\pi^-]$. The best-fit line shapes for ϕ, $\Lambda(1520)$, and nonresonant K^+K^-p well reproduce the K^+K^- and the K^-p mass spectra, as shown in Fig. 2. The χ^2 probability $P(\chi^2; \mathrm{ndf})$ is quoted in each of the fitted K^+K^- and K^-p mass spectra, where ndf represents the number of degrees of freedom. The fits with Monte Carlo line shapes were based on the events beyond the $\phi - \Lambda(1520)$ interference region in which the two resonances appear. The fit results were then interpolated into the interference region, keeping the magnitudes of Monte Carlo line shapes as determined from the fit [21]. This simultaneous fit with Monte Carlo line shapes is a self-consistent method to reproduce the measured K^+K^- and K^-p mass spectra, which pertains to the further study of interference effects.

Forward differential cross sections for ϕ and $\Lambda(1520)$ production channels were measured using the best-fit results with Monte Carlo line shapes in the ϕ and $\Lambda(1520)$ mass bands except for the interference region. The forward differential cross sections ($d\sigma/dt$ at $t = t_{\mathrm{min}}$) for ϕ photoproduction are compared with previous results from LEPS [8] near the threshold, as shown in Fig. 3(left). Thus, we reconfirmed the existence of the bump structure around $E_\gamma = 2.0$ GeV. The structure appears persistent even with different ϕ-mass bands, different slope parameters, and the exclusion of the interference region in which ϕ and $\Lambda(1520)$ mass bands overlap. The slope parameters of the $|t - t_{\mathrm{min}}|$ distributions decreased as the photon energy increased. The forward cross sections were obtained

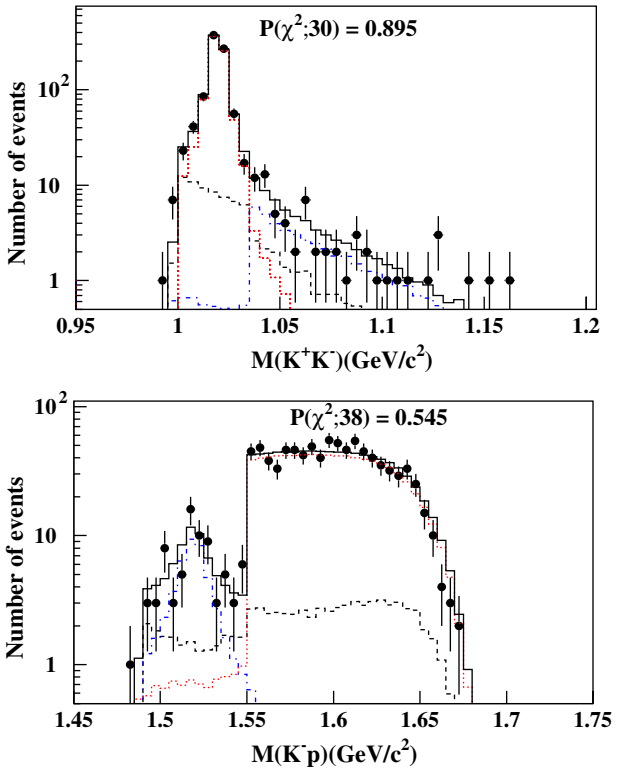

FIG. 2. The invariant mass spectra for (top) K^+K^- and (bottom) K^-p systems are displayed as closed circles for forward K^+K^- events in the energy region from 1.973 to 2.073 GeV, respectively. The best-fit line shapes for ϕ are overlaid with dotted lines, while those for $\Lambda(1520)$ are represented as dot-dashed lines. Dashed lines represent the contributions of nonresonant K^+K^-p production.

from the fit with linearly energy-dependent slope parameters $[d\sigma/dt = d\sigma/dt|_{t=t_{\mathrm{min}}} \exp(-b|t - t_{\mathrm{min}}|)$, where $b = -(11.47 - 3.47E)$ GeV$^{-2}]$ and E is a dimensionless quantity taken from the value of the photon energy in GeV.

Figure 3 (right) shows the differential cross sections for $\Lambda(1520)$ photoproduction in the angular regions of $0.9 < \cos\theta^*_{K^+} < 1.0$ and the comparison of the previous LEPS results by Kohri *et al.* [22]. While the previous

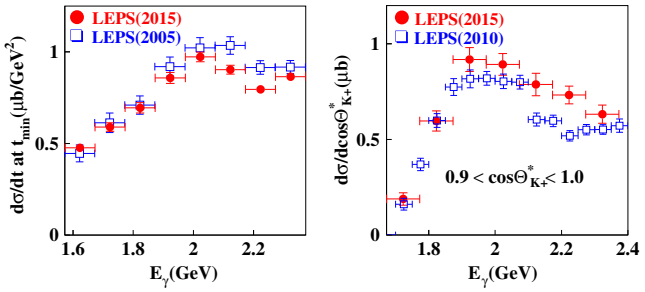

FIG. 3. Forward differential cross sections for (left) ϕ and (right) $\Lambda(1520)$ photoproduction. Open squares represent cross-section results obtained without considering interference, while solid circles represent new measurement results.

analysis was based on events with a single K^+ track, the new analysis required at least two tracks among K^-, K^+, and p. As a result, the event statistics in this measurement at forward K^+ angles were smaller than those from the previous analysis. Though the statistics were low, both results are in good agreement with the earlier analysis and feature the bump structure near $E_\gamma = 2$ GeV. Interestingly, the two cross-section results show the bump structure at the same E_γ, which could indicate a strong correlation between the ϕ and $\Lambda(1520)$. However, the difference between the cross sections obtained with and without the interference region is not large enough to account for the bump structure.

The differential cross sections for the $\gamma p \to K^+K^-p$ reaction can be decomposed into

$$\frac{d^2\sigma}{dm_{K^+K^-}dm_{K^-p}} \propto |\mathcal{M}_\phi + \mathcal{M}_{\Lambda(1520)} + \mathcal{M}_{\rm nr}|^2, \quad (1)$$

where $\mathcal{M}_\phi$ and $\mathcal{M}_{\Lambda(1520)}$ are the complex amplitudes for ϕ and $\Lambda(1520)$ production processes, respectively. $\mathcal{M}_{\rm nr}$ represents nonresonant K^+K^-p production. Each complex amplitude includes individual amplitudes for all possible subprocesses, such as Pomeron-exchange and pseudoscalar meson-exchange processes for ϕ photoproduction. However, log-likelihood fits of the data in ϕ and $\Lambda(1520)$ bands excluding the ϕ and $\Lambda(1520)$ interference region ($|\mathcal{M}_\phi + \mathcal{M}_{\rm nr}|^2$) with Monte Carlo line shapes ($|\mathcal{M}_\phi|^2 + |\mathcal{M}_{\rm nr}|^2$) result in the χ^2 probability $P(\chi^2) > 0.2$ in most cases. Moreover, the S-P wave interference in ϕ photoproduction is known to be as small as 1% [23]. Therefore, we assume that $|\mathcal{M}_\phi + \mathcal{M}_{\Lambda(1520)} + \mathcal{M}_{\rm nr}|^2 \approx |\mathcal{M}_\phi + \mathcal{M}_{\Lambda(1520)}|^2 + |\mathcal{M}_{\rm nr}|^2$, where the interference terms between $\mathcal{M}_{\rm nr}$ and two resonance amplitudes are neglected. The contribution from the term $|\mathcal{M}_{\rm nr}|^2$ was then subtracted from the data.

The differential cross sections for the $\gamma p \to K^+K^-p$ reaction via the ϕ and $\Lambda(1520)$ resonances can be written as [24]

$$\left.\frac{d^2\sigma}{dm_{K^+K^-}dm_{K^-p}}\right|_{\phi,\Lambda(1520)} \propto |\mathcal{M}_\phi + \mathcal{M}_{\Lambda(1520)}|^2 = \left|\frac{ae^{i\psi_a}}{m_\phi^2 - m_{K^+K^-}^2 + im_\phi\Gamma_\phi} + \frac{be^{i\psi_b}}{m_{\Lambda^*}^2 - m_{K^-p}^2 + im_{\Lambda^*}\Gamma_{\Lambda^*}}\right|^2, \quad (2)$$

where a and b denote the magnitudes of the Breit-Wigner amplitudes for ϕ and $\Lambda(1520)$, respectively. Here ψ_a and ψ_b represent phases for ϕ and $\Lambda(1520)$ production amplitudes, respectively. We integrate the differential cross sections over the K^-p mass interval in the ϕ-$\Lambda(1520)$ interference region, assuming that the phase ψ_b is constant in the interference region for each energy interval. The integrated cross sections can then be given by

$$\frac{d\sigma}{dm} \propto \left|\frac{ae^{i\psi_a}}{m_\phi^2 - m^2 + im_\phi\Gamma_\phi} + B(m)e^{i\psi_b}\right|^2, \quad (3)$$

where m denotes $m_{K^+K^-}$. $|B(m)|^2$ corresponds to the Breit-Wigner line shape of $\Lambda(1520)$ projected onto the K^+K^- mass axis in the interference region. The interference term $I(m)$ between the two amplitude terms can be obtained as [25]

$$I(m) = 2|aB(m)|\frac{(m_\phi^2 - m^2)\cos\psi + \Gamma_\phi m_\phi \sin\psi}{(m_\phi^2 - m^2)^2 + m_\phi^2\Gamma_\phi^2}, \quad (4)$$

where $\psi = |\psi_a - \psi_b|$ is the relative phase between the phases ψ_a and ψ_b.

For the relative phase between the ϕ and $\Lambda(1520)$ amplitudes, we fitted data in the interference region with Eq. (4). Here, the relative amplitudes of a and $B(m)$ for each energy interval are fixed from a simultaneous fit utilizing Monte Carlo line shapes in the ϕ and $\Lambda(1520)$ mass bands except for the interference region. Consequently, only a single parameter, the relative phase ψ, exists in the fit. The best-fit results for the relative phase are shown as solid curves in Fig. 4. To verify the reliability of this approach, the fit results are compared with theoretical estimates based on the effective Lagrangian approach [26], taking the ϕ and $\Lambda(1520)$ production amplitudes into account. The reaction dynamics is represented by the invariant amplitudes and form factors in this theoretical approach. The phase of $\psi = \pi/2$ was chosen for simplicity. The theoretical estimates for the maximum

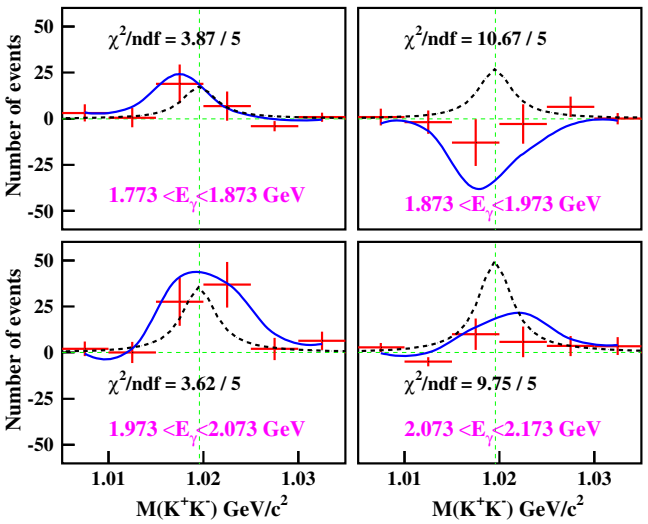

FIG. 4. Difference between event yields in the interference region and the sum of ϕ and $\Lambda(1520)$ events for forward K^+K^- events, in four 0.1-GeV-wide energy regions from 1.773 to 2.173 GeV. The best-fit results for the relative phase are overlaid with solid curves, while dashed lines are from theoretical estimates assuming maximum constructive ϕ-$\Lambda(1520)$ interference with $\psi = \pi/2$.

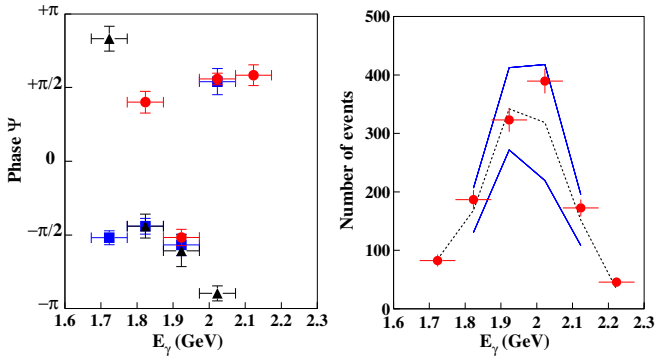

FIG. 5. (Left) Phase angles for K^+K^- (circles), K^-p (squares), and K^+p (triangles) events. (Right) Integrated yields (when K^+K^- pairs are detected at forward angles) in the interference region (circles) compared to the predicted levels for the maximum and minimum bounds (solid lines). The dashed line indicates the predicted levels for no ϕ-$\Lambda(1520)$ interference.

constructive ϕ-$\Lambda(1520)$ interference are shown as dashed curves in Fig. 4, which are consistent with those predicted by Eq. (4).

The fit results for relative phase are represented in Fig. 5(left). The χ^2 probability was required to exceed 0.1%. For forward K^-p and K^+p events, the energy regions between 1.673 and 2.073 GeV are explored. The maximum constructive interference has $\psi = \pi/2$, while the maximum destructive interference is represented by $\psi = -\pi/2$. For K^+K^- events detected in the forward directions, the resulting relative phases are in most cases constructive, while those for forward $K^\pm p$ events are destructive.

For forward K^+K^- events in the energy region of $1.973 < E_\gamma < 2.073$ GeV, the integrated event yield in the interference region approaches close to the maximum bound for the ϕ-Λ interference, as shown in Fig. 5 (right), which is consistent with the relative phase $\psi = 1.69 \pm 0.12$ rad. Moreover, the relative phase flips its sign as a function of photon energy E_γ. For K^-p events, the relative phase in the energy region of $1.973 < E_\gamma < 2.073$ GeV firmly stays at a positive value, while in other energy regions it supports destructive interference. Thus, it can be inferred that a change in interference patterns occurs when K^-p is studied at forward angles. For the K^+p events, only in the lowest-energy region does the phase appears in the positive side, but it remains close to π, which corresponds to zero interference.

Different phases for different event modes (forward K^+K^-, K^-p, and K^+p events) may arise from differing kinematic coverages for the photoproduction of ϕ and $\Lambda(1520)$. We relate the phases near $\pi/2$ for forward K^+K^- events to the interference between the Pomeron-exchange amplitude for ϕ and the K-exchange amplitude for $\Lambda(1520)$ photoproduction. For forward proton events (K^-p and K^+p), unnatural-parity exchange processes become important in ϕ photoproduction. However, it is worth noting that the ϕ-$\Lambda(1520)$ interference effect does not account for the 2.1-GeV bump structure in forward differential cross sections for ϕ photoproduction. This result is consistent with a recent report from CLAS regarding the $\Lambda(1520)$ effect [10]. The energy dependence of the phase may indicate nontrivial rescattering contributions from other hyperon resonances. The bump structure could then be associated with either rescattering processes due to kinematic overlap in phase space or exotic structures involving a hidden-strangeness pentaquark state and the exchange of a new Pomeron. Alternatively, they could be due to a combination of both factors.

In summary, the photoproduction of the $\gamma p \to K^+K^-p$ reaction was measured using the LEPS detector at energies from 1.57 to 2.40 GeV. The ϕ-$\Lambda(1520)$ interference measurement is a good probe to study the origin of enhanced production cross sections for ϕ and $\Lambda(1520)$ near $\sqrt{s} = 2.1$ GeV. In this Letter, we presented relative phases between ϕ and $\Lambda(1520)$ production amplitudes by using a two-dimensional mass fit with Monte Carlo line shapes. We reconfirmed the bump structure in the analysis without the ϕ-$\Lambda(1520)$ interference region. On the other hand, we observed clear ϕ-$\Lambda(1520)$ interference effects in the energy range from 1.673 to 2.173 GeV. The data obtained in the present study provide the first-ever experimental evidence for the ϕ-$\Lambda(1520)$ interference effect in ϕ photoproduction. The relative phases suggest strong constructive interference for K^+K^- pairs observed at forward angles, while destructive interference results from the emission of protons at forward angles. The nature of the bump structure could originate from interesting exotic structures such as a hidden-strangeness pentaquark state, a new Pomeron exchange, or rescattering processes via other hyperon states.

The authors gratefully acknowledge the contributions of the staff of the SPring-8 facility. Thanks are due to A. Hosaka for invaluable theoretical discussions. This research was supported in part by the U.S. National Science Foundation, the Ministry of Education, Science, Sports and Culture of Japan, the National Science Council of the Republic of China, the National Research Foundation of Korea, Korea University, and Pukyong National University.

*Also at Research Center for Nuclear Physics, Osaka University, Ibaraki, Osaka 567-0047, Japan.

[1] A. I. Titov, T.-S. H. Lee, H. Toki, and O. Streltsova, Phys. Rev. C **60**, 035205 (1999).
[2] A. I. Titov, T. Nakano, S. Daté, and Y. Ohashi, Mod. Phys. Lett. A **23**, 2301 (2008).
[3] D. Schildknecht, Acta Phys. Pol. B **37**, 595 (2006).
[4] A. Sibirtsev, H. W. Hammer, U. G. Meissner, and A. W. Thomas, Eur. Phys. J. A **29**, 209 (2006).

[5] J.-M. Laget, Phys. Lett. B **489**, 313 (2000).
[6] A. Donnachie, H. G. Dosch, P. V. Landshoff, and O. Natchmann, *Pomeron Physics and QCD* (Cambridge University Press, Cambridge, England, 2002).
[7] A. Donnachie and P. V. Landshoff, Nucl. Phys. **B244**, 322 (1984).
[8] T. Mibe *et al.* (LEPS Collaboration), Phys. Rev. Lett. **95**, 182001 (2005).
[9] H. Seraydaryan *et al.* (CLAS Collaboration), Phys. Rev. C **89**, 055206 (2014).
[10] B. Dey *et al.* (CLAS Collaboration), Phys. Rev. C **89**, 055208 (2014).
[11] A. Kiswandhi, J.-J. Xie, and S. N. Yang, Phys. Lett. B **691**, 214 (2010).
[12] R. Aaij *et al.* (LHCb Collaboration), Phys. Rev. Lett. **115**, 072001 (2015).
[13] S. Ozaki, A. Hosaka, H. Nagahiro, and O. Scholten, Phys. Rev. C **80**, 035201 (2009).
[14] H-Y. Ryu, A. I. Titov, A. Hosaka, and H-Ch. Kim, Prog. Theor. Exp. Phys. **2014**, 23D03 (2014).
[15] N. Muramatsu *et al.*, Nucl. Instrum. Methods Phys. Res., Sect. A **737**, 184 (2014).
[16] T. Nakano *et al.*, Nucl. Phys. **A670**, 332 (2000); **A721**, C112 (2003).
[17] K. A. Olive *et al.* (Particle Data Group), Chin. Phys. C **38**, 090001 (2014).
[18] W. C. Chang *et al.*, Phys. Rev. C **82**, 015205 (2010).
[19] J. Y. Chen, Ph.D. thesis, National Sun Yat-sen University, 2009.
[20] S. H. Hwang *et al.* (LEPS Collaboration), Phys. Rev. Lett. **108**, 092001 (2012).
[21] S. Y. Ryu, Ph.D. thesis, Osaka University, 2015.
[22] H. Kohri *et al.* (LEPS Collaboration), Phys. Rev. Lett. **104**, 172001 (2010).
[23] D. C. Fries, P. Heine, H. Hirschmann, A. Markou, E. Seitz, H.-J. Behrend, W. P. Hesse, W. A. McNeely, and T. Miyachi, Nucl. Phys. **B143**, 408 (1978).
[24] H. Ejiri, P. Richard, S. Ferguson, R. Heffner, and D. Perry, Phys. Rev. Lett. **21**, 373 (1968); H. Ejiri and J. P. Bondorf, Phys. Lett. B **28**, 304 (1968); H. Ejiri, P. Richard, S. Ferguson, R. Heffner, and D. Perry, Nucl. Phys. **A128**, 388 (1969).
[25] Y. Azimov, J. Phys. G **37**, 023001 (2010).
[26] See S. i. Nam *et al.* (to be published) for the theoretical calculation approach.